

Supplementary Information for

Lattice-Matching Ni-Based Scaffold with Spongy Cover for Uniform Electric Field against Lithium Dendrite

*Yunhao Zhao**^a; Rui Xu**^a; Yuanyuan Zhou^a; Fangzheng Wang^a; Cheng Tong^a;*

Minhua Shao^b; Meng Wang^a; Cunpu Li*^a; and Zidong Wei^a*

^a The State Key Laboratory of Power Transmission Equipment & System
Security and New Technology, Chongqing Key Laboratory of Chemical Process
for Clean Energy and Resource Utilization, School of Chemistry and Chemical
Engineering, Chongqing University, Shazhengjie 174, Chongqing 400044, China.

lcp@cqu.edu.cn; wmeng@cqu.edu.cn

^b Department of Chemical and Biological Engineering, Hong Kong University
of Science and Technology, Clear Water Bay, Kowloon, Hong Kong, China.

* To whom correspondence should be addressed.

** Yunhao Zhao and Rui Xu contributed equally.

Experimental Session:

H₂BDC, Ni(NO₃)₂·6H₂O, CO(NH₂)₂, Ni foam (NF) and DMF are purchased from Aladdin, Shanghai. All the chemicals were directly used after purchase without further purification.

Synthesis of NiO@NF: NF was cut into 2mm x 5mm pieces before washed with nitric acid (1:1), water and ethanol, subsequently, to remove the oxide layer on the surface. Ni(NO₃)₂·6H₂O (0.68g) and CO(NH₂)₂ (0.75g) were dissolved in 50 mL ethanol and stirred for 20 min until transparent solution was formed. The solution was then sealed into a Teflon-lined autoclave with NF and kept at 120°C for 6 hours. After that, the NF was washed under water and ethanol subsequently, followed by heating in a tube oven at 350°C under N₂ atmosphere for 2 hours. The product was considered as NiO@NF.^{1, 2}

Synthesis of CNS@NF: H₂BDC (0.4984g, 3 mmol), Ni(NO₃)₂·6H₂O (0.4362g, 1.5 mmol) were dissolved in 50 mL DMF and stirred for 20 min, resulting in a green, transparent solution, which were once again sealed into a Teflon-lined autoclave with NiO@NF and kept at 150°C for 12 hours. The NF was washed under water and ethanol subsequently and kept at 500°C in a tube oven under N₂ atmosphere for 2 hours. The product was considered as CNS@NF.^{3, 4}

Material characterization: To investigate the crystal structure of CNS@NF, powdered Ni-BDC MOF and NiO were also deposited by the same hydrothermal process onto NF respectively. Three crystals were obtained by scratching the surface of the respective NF to be characterized by transmission electron microscopy (TEM), powdered X-ray diffraction (XRD), and X-ray photoelectron spectroscopy (XPS). XRD pattern was recorded on a Rigaku D/max 2200 pc diffractometer, with Cu K α radiation of wavelength $\lambda = 0.15418$ nm, at 40 kV and 40 mA, and XPS (Thermo Scientific K-Alpha) with Al K α sources ($h\nu = 1486.6$ eV) was used to confirm the product is the same as predicted. The microstructure was characterized by scanning electron microscopy (SEM, Hitachi S-4800) and TEM (JEOL JEM 2100F) with energy dispersive spectrum (EDS, OXFORD X-MAX). Thermo-gravimetric analysis (TGA) was performed under nitrogen atmosphere on an SDT Q600 instrument.

Lattice mismatch (f) calculation: lattice mismatch (f) is a crucial factor to dictate the mode of epitaxial growth. The following equation is given to provide the definition of f, where α_s and α_g are the original lattice constants of the seed and overgrowth material, respectively.⁵

$$f = \frac{\alpha_s - \alpha_g}{\alpha_s}$$

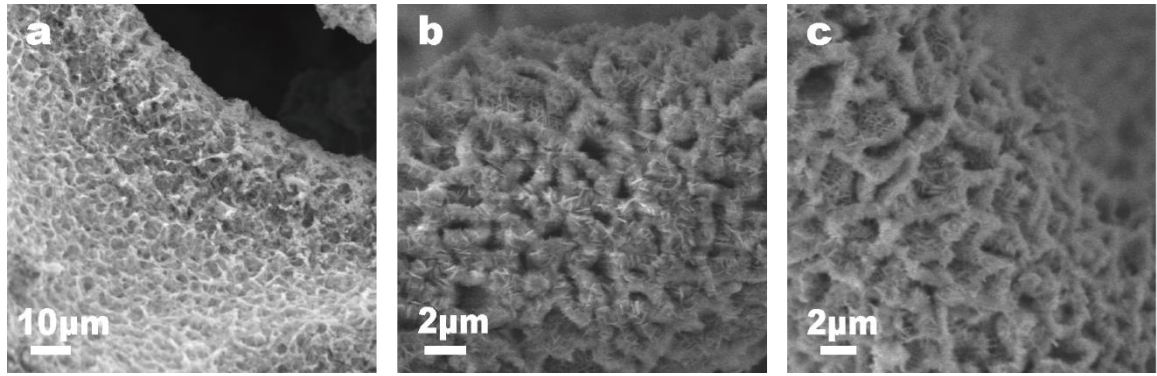
Preparation of the C-S composites: The C-S composites were prepared via a melt-diffusion process. Sublimed sulfur and carbon black (Super-P) were mixed uniformly by ball milling, which was then annealed at 155°C under a N₂ atmosphere for 24 h. TGA was used to determine the mass ratio of S in the composite.⁶

Electrochemical measurement: Electrochemical characterization was carried out using 2032 type coin cells assembled under Ar atmosphere glovebox with O₂ and H₂O both under 1 ppm. For all the

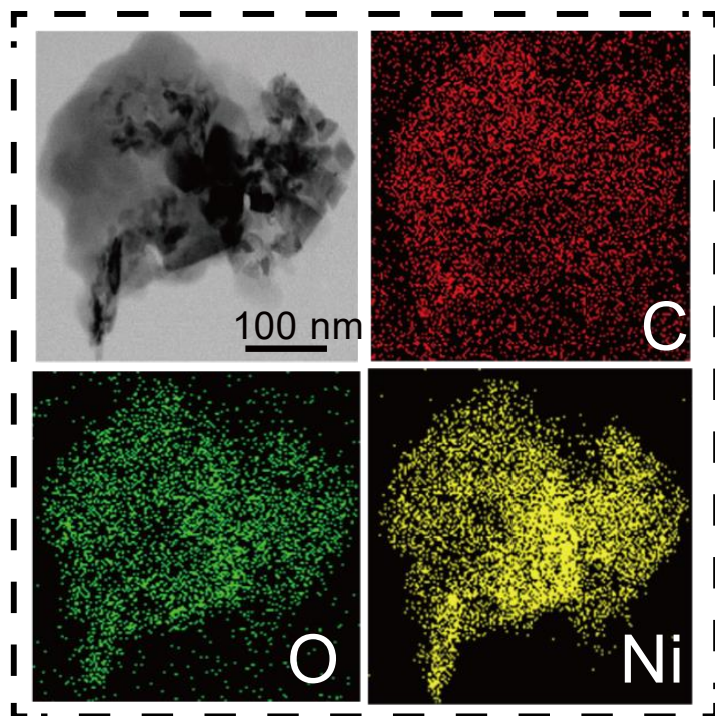
battery assembly, 60 μL of electrolyte was used for each cell. The as obtained CNS@NF, long side with pristine Li, was directly used as anode during the assembly of symmetric cells. 1.0 M lithium bis(trifluoromethanesulfonyl)imide (LiTFSI) salt dissolved in a hybrid solution of 1,3-dioxolane and dimethoxymethane (1:1 in volume) with 1 wt% LiNO_3 as an additive was used as electrolyte. Li foil was used as the counter/reference electrode. Then, 12 $\text{mAh}\cdot\text{cm}^{-2}$ of Li was plated onto the CNS@NF and pristine Li at a current density of 1 $\text{mA}\cdot\text{cm}^{-2}$ on a battery system (LAND, China) to get Li@CNS@NF. The galvanostatic charge-discharge (GCD) tests were carried on the same system. Electrochemical impedance spectroscopy (EIS) was conducted on a Princeton 1260A Impedance Analyzer by applying a sine wave with an amplitude of 10 mV over a frequency range of 100 kHz to 10 mHz. Symmetric cells cycled for specific number of hours were disassembled and pristine Li and Li@CNS@NF, respectively, were characterized by SEM. To test the stability of Li stripping/plating process, cells comprising Cu and CNS@NF as anode, respectively, were assembled accordingly and Li foil was used as counter/reference electrode. The as obtained cells were activated by scanning in the voltage window of 0-1V at current density of 1 $\text{mA}\cdot\text{cm}^{-2}$ five times, followed by electrochemical disposition of 2 $\text{mAh}\cdot\text{cm}^{-2}$ of Li. The Li stripping/plating tests were then conducted by stripping Li until the voltage reached 1V and depositing 1 $\text{mAh}\cdot\text{cm}^{-2}$ of Li subsequently. For each cycle, coulombic efficiency was calculated. For Li//S cells assembly, the testing sulfur cathodes were fabricated by mixing Super-P, C-S composite and polyvinylidene fluoride (PVDF) at weight ratio of 1:8:1, followed by dissolving the mixture in the N-methyl-2-pyrrolidone (NMP) solvent. The as obtained slurry was then blade cast onto aluminum foil. The same electrolyte was employed with Li@CNS@NF and pristine Li as counter/reference electrode. The galvanostatic discharge/charge test was performed on a battery system (LAND, China) in the voltage window of 1.6–2.8 V for Li//S batteries at room temperature. The testing LFP cathodes were fabricated by mixing Super-P, lithium iron phosphate (LFP) and PVDF at weight ratio of 1:8:1 by ball milling, followed by dissolving the mixture in the N-methyl-2-pyrrolidone (NMP) solvent. The as obtained slurry was then blade cast onto aluminum foil. 1.0 M LiPF_6 in ethylene carbonate (EC) and diethyl carbonate (DEC) (v:v = 1:1) was used as electrolyte for Li//LFP cells and Li@CNS@NF and pristine Li was used, respectively, as counter/reference electrode. The voltage window of 2.4-4.0V for Li//LFP was used during GCD testing.

Coulombic efficiency (CE) calculation: CE was calculated using the following formula to determine the charge efficiency by which electrons are transferred in batteries, whereas $C_{\text{discharge}}$ and C_{charge} refer to the capacity during discharge and charge, respectively.

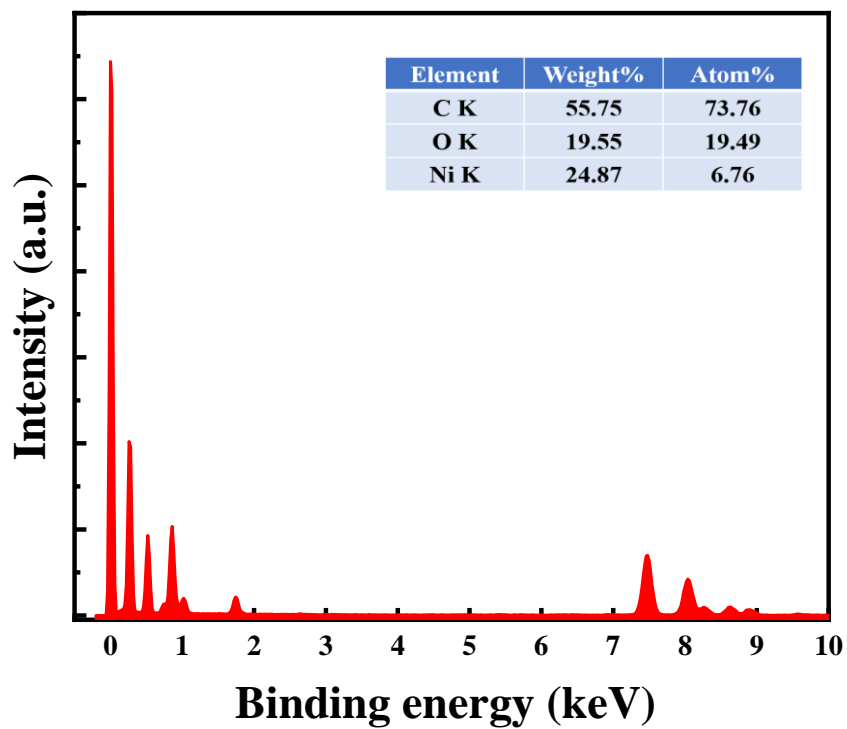
$$CE = \frac{C_{\text{discharge}}}{C_{\text{charge}}}$$



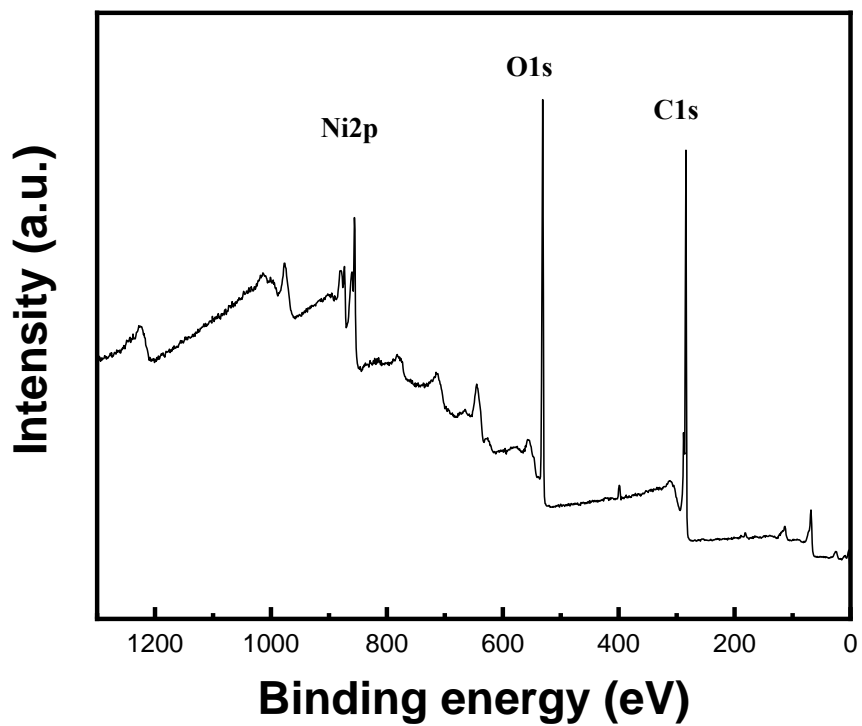
Supplementary Fig. 1. Additional SEM image of a) NiO@NF b,c) CNS@NF



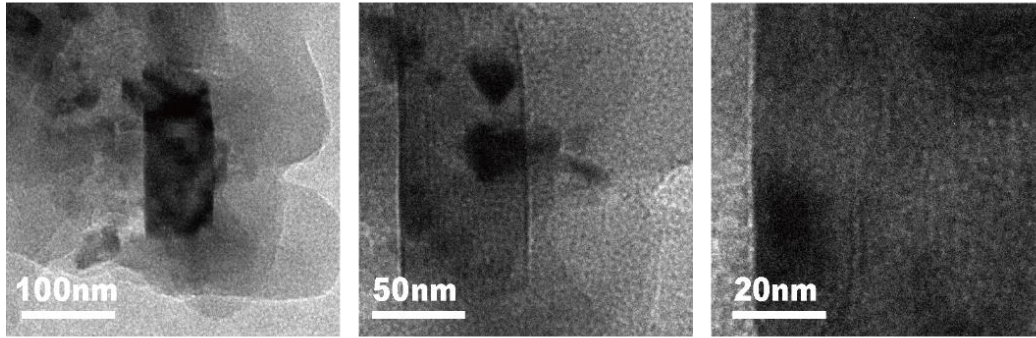
Supplementary Fig. 2. Typical elemental mapping of CNS, scratched from the surface of CNS@NF



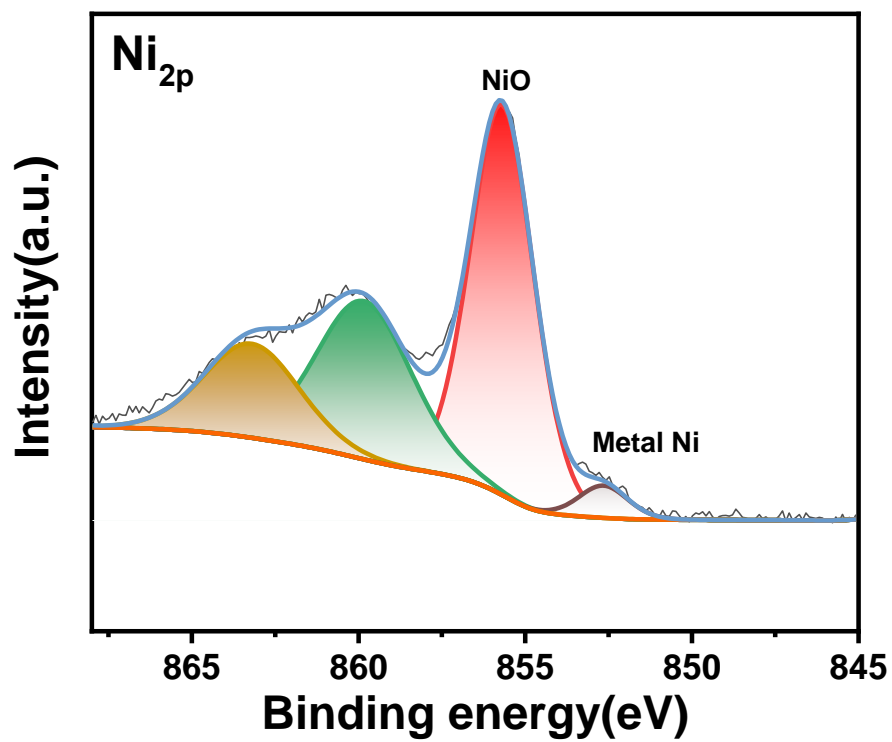
Supplementary Fig. 3. EDS spectrum of CNS@NF powder, with the table summarized of weight and atom percentage of elements in CNS@NF



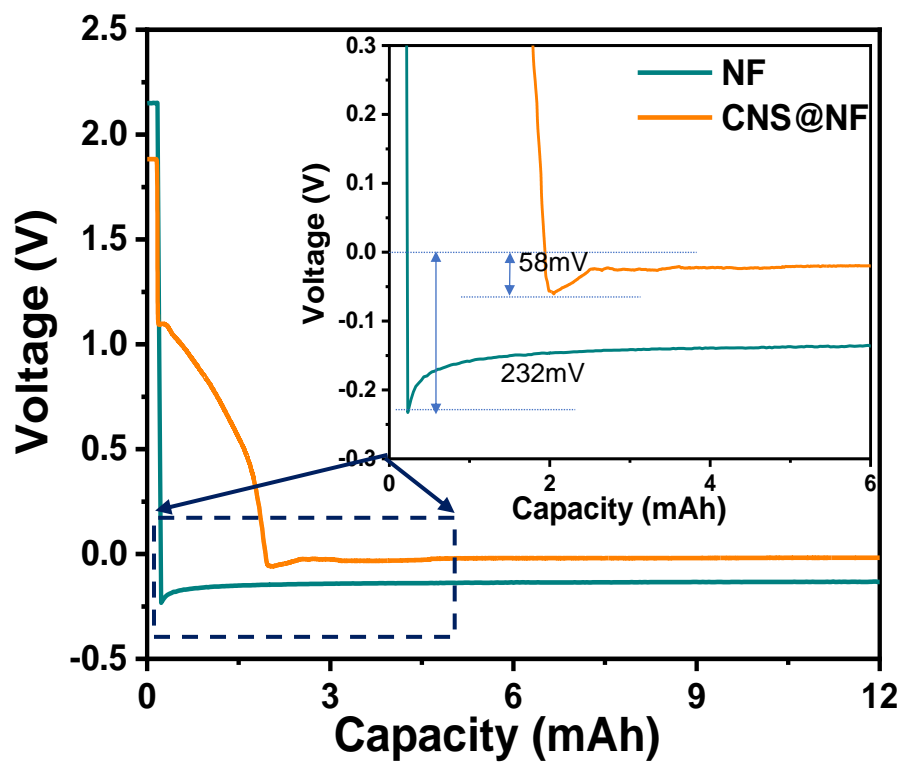
Supplementary Fig. 4. Full XPS spectrum of CNS@NF and its peak attribution. This result is consistent with the elemental mapping and EDS spectrum of CNS@NF.



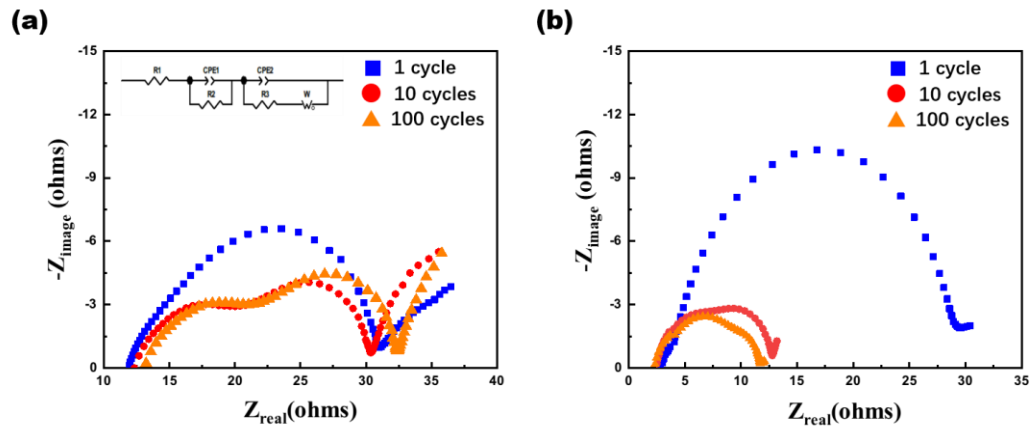
Supplementary Fig. 5. Additional TEM image of CNS@NF TEM image with different amplification factor, which clearly shows the desirable thin nanosheet structure.



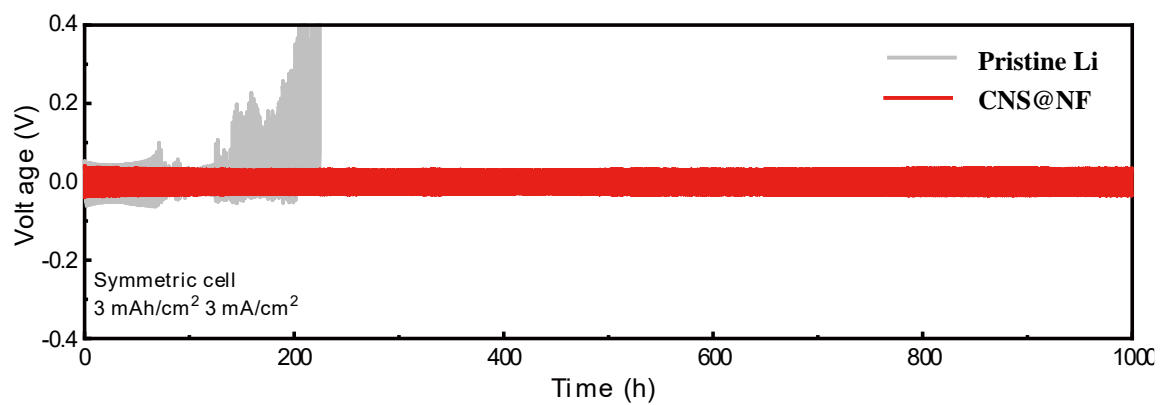
Supplementary Fig. 6. Ni region of XPS spectrum of CNS@NF and its peak attribution.



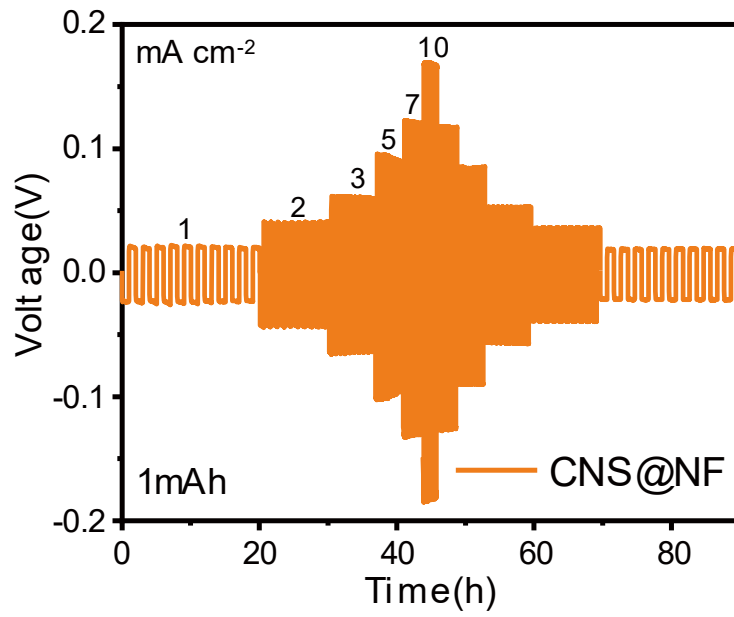
Supplementary Fig. 7. Voltage-time curve during the electrodeposition process ($1 \text{ mA}\cdot\text{cm}^{-2}$). Smaller overpotential was spotted indicating its good electroconductivity, and during the first two hours the potential of cells with CNS@NF dropped more slowly than cells with NF, indicating transformation happening.



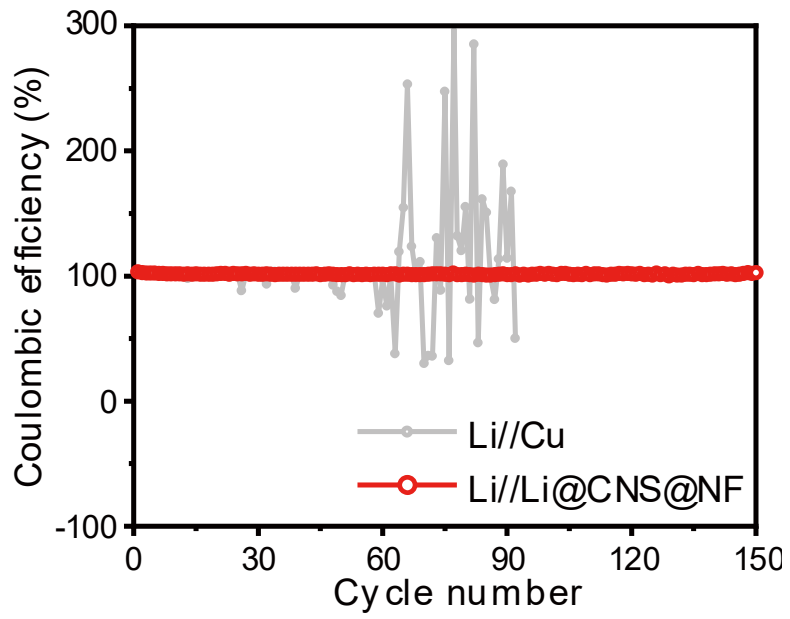
Supplementary Fig. 8. EIS nyquist plot of a) Li-Li@CNS@NF symmetric cells and b) Li-pristine Li symmetric cells, after 1st, 10th, 100th cycle, respectively. R_1 , R_2 , R_3 in the equivalent circuit represent resistance from electrolyte (R_b), resistance from SEI (R_{SEI}) and resistance from the charge transfer (R_{ct}) as shown in Table S1.⁷ Symmetric cells after 1, 10, 50 cycles of GCD testing were measured, and both the R_{SEI} and R_{ct} , represented by the two semi-circles, hardly changed between the 50th cycles and the 100th cycles, indicating good SEI stability. Two semi-circles can be seen after 50th and 100th cycles, but not after the first cycles, indicating the presence of SEI. The R_{ct} of Li-pristine Li cells become significantly smaller after cycling, owing to the increased surface area caused by the dendrite formation.



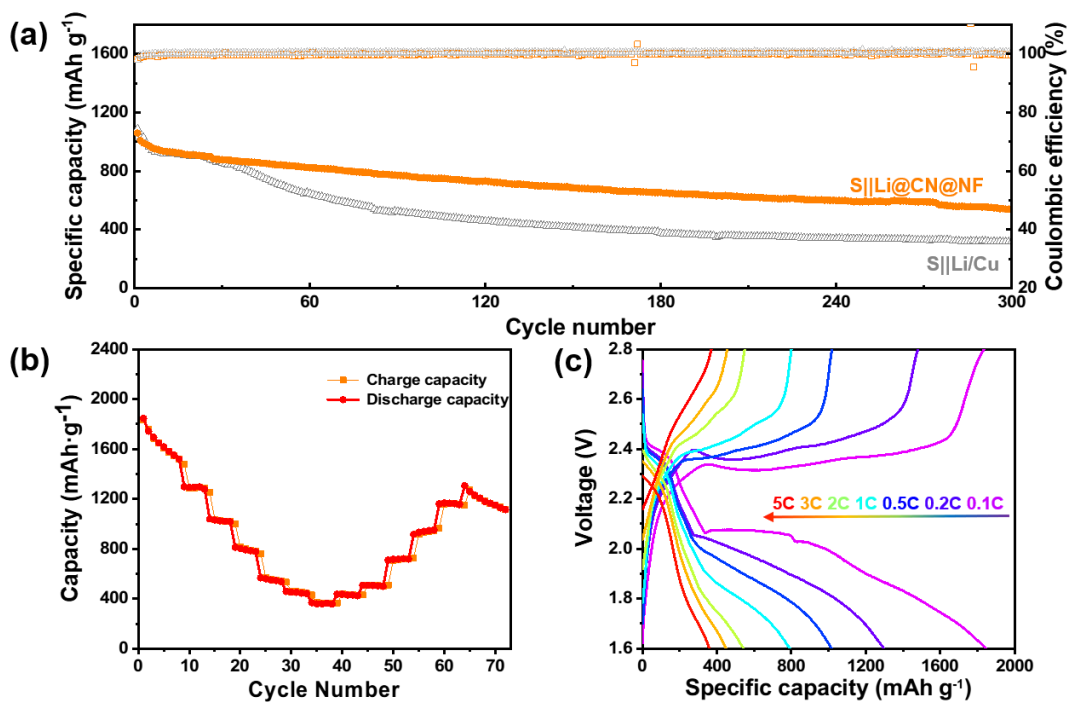
Supplementary Fig. 9. Li-Li@CNS@NF symmetric cells cycling performance at current density of $3 \text{ mA}\cdot\text{cm}^{-2}$. It shows in the picture that the overpotential remains rather small after long time (1000 hours) cycling.



Supplementary Fig. 10. Rate performance of cells comprising CNS@NF at current density from 1 mA·cm⁻² to 10 mA·cm⁻²



Supplementary Fig. 11. CE of the Li stripping/plating process of Li//Li@CNS@NF cells, with Li//Cu cells as comparison



Supplementary Fig. 12. Li-S cells electrochemical performance. a) cycling stability of pristine Li//S and Li@CNS@NF//S full cells at 0.5C ($1C=1678\text{ mA}\cdot\text{h}\cdot\text{g}^{-1}$). Although the polysulfides shuttling effect tremendously influenced the performance of both cells, the capacity of cells with pristine Li dropped much faster after the initial cycles, which was thought to result from the severe polarization caused by side reactions on the raw Li anode. b) rate performance of Li@CNS@NF//S at 0.1C, 0.2C, 0.5C, 1C, 2C, 3C, 5C and c) the corresponding voltage profiles.

Supplementary Table 1. Cycling life performance comparison table of Li@CNS@NF with other reported Li anode materials.

Material name	Current density (mA·cm ⁻²)	Cycling capacity (mAh·cm ⁻²)	Time(h)	Reference
Li-coated PI	5	1	~38.89	8
Li/C-wood	3	1	150	9
Li@CC	5	1	~77.78	10
Ti ₃ C ₂ -LiB-Li	1	1	1000	11
Zn-MXene-Li	1	1	1200	12
Mg@C60@Li	1	1	550	13
Li-CF/Ag	1	1	400	14
NGCF@Li	3	1	600	15
Li/C3N4/CC	2	2	1500	16
Li@NRA-CC	1	1	1200	17
ZMNF	5	2	300	18
NPAuLi ₃ @NF	2	2	1400	19
Li@CNS@NF	1	1	1500	This work
	3	3	1000	
	5	5	1000	

Supporting information reference

1. S. Ding, T. Zhu, J. S. Chen, Z. Wang, C. Yuan and X. W. Lou, *Journal of Materials Chemistry*, 2011, **21**, 6602-6606.
2. M. Huang, F. Li, J. Y. Ji, Y. X. Zhang, X. L. Zhao and X. Gao, *CrystEngComm*, 2014, **16**, 2878-2884.
3. T. Noor, N. Zaman, H. Nasir, N. Iqbal and Z. Hussain, *Electrochimica Acta*, 2019, **307**, 1-12.
4. Z. Zhang, Y. Chen, S. He, J. Zhang, X. Xu, Y. Yang, F. Nosheen, F. Saleem, W. He and X. Wang, *Angewandte Chemie International Edition*, 2014, **53**, 12517-12521.
5. J. Liu and J. Zhang, *Chemical Reviews*, 2020, **120**, 2123-2170.
6. R. Gan, N. Yang, Q. Dong, N. Fu, R. Wu, C. Li, Q. Liao, J. Li and Z. Wei, *Journal of Materials Chemistry A*, 2020, **8**, 7253-7260.
7. S. S. Zhang, K. Xu and T. R. Jow, *Electrochimica Acta*, 2006, **51**, 1636-1640.
8. Y. Liu, D. Lin, Z. Liang, J. Zhao, K. Yan and Y. Cui, *Nature Communications*, 2016, **7**, 10992.
9. Y. Zhang, W. Luo, C. Wang, Y. Li, C. Chen, J. Song, J. Dai, E. M. Hitz, S. Xu, C. Yang, Y. Wang and L. Hu, *Proceedings of the National Academy of Sciences*, 2017, **114**, 3584.
10. Y. Zhou, Y. Han, H. Zhang, D. Sui, Z. Sun, P. Xiao, X. Wang, Y. Ma and Y. Chen, *Energy Storage Materials*, 2018, **14**, 222-229.
11. Z. Zhao and B. Li, *Electrochimica Acta*, 2021, **365**, 137341.
12. J. Gu, Q. Zhu, Y. Shi, H. Chen, D. Zhang, Z. Du and S. Yang, *ACS Nano*, 2020, **14**, 891-898.
13. Q. Xu, J. Lin, C. Ye, X. Jin, D. Ye, Y. Lu, G. Zhou, Y. Qiu and W. Li, *Advanced Energy Materials*, 2020, **10**, 1903292.
14. R. Zhang, X. Chen, X. Shen, X.-Q. Zhang, X.-R. Chen, X.-B. Cheng, C. Yan, C.-Z. Zhao and Q. Zhang, *Joule*, 2018, **2**, 764-777.
15. L. Liu, Y.-X. Yin, J.-Y. Li, S.-H. Wang, Y.-G. Guo and L.-J. Wan, *Advanced Materials*, 2018, **30**, 1706216.
16. Y. Xu, T. Li, L. Wang and Y. Kang, *Advanced Materials*, 2019, **31**, 1901662.
17. B. Yu, T. Tao, S. Mateti, S. Lu and Y. Chen, *Advanced Functional Materials*, 2018, **28**, 1803023.
18. C. Sun, Y. Li, J. Jin, J. Yang and Z. Wen, *Journal of Materials Chemistry A*, 2019, **7**, 7752-7759.
19. Y. Liang, Y. Chen, X. Ke, Z. Zhang, W. Wu, G. Lin, Z. Zhou and Z. Shi, *Journal of Materials Chemistry A*, 2020, **8**, 18094-18105.